

High Resolution Terrestrial Laser Scanning for Tunnel Deformation Measurements

Timothy NUTTENS, Alain DE WULF, Lander BRAL, Bart DE WIT, Leen CARLIER, Marijke DE RYCK, Cornelis STAL, Denis CONSTALES, Hans DE BACKER, Belgium

Key words: Terrestrial laser scanning, tunnels, deformation measurements

SUMMARY

By delivering millions of very accurate 3D points, laser scanning is an alternative for classical topographical measurements with a total station or digital photogrammetry for measurements in difficult field conditions. This makes terrestrial high resolution laser scanning a technique that is increasingly being used for geodetic deformation measurements of civil technical constructions, i.c. newly built tunnels. This paper deals with the error values during processing of a measured tunnel section and the final determination of the deformations of this tunnel section based on 3D laser scan point clouds.

The subject of this research is the still ongoing construction of two railway tunnels under Brussels Airport (Zaventem, Belgium). There are two times six tunnel sections that have to be closely monitored. These tunnel sections have to be scanned immediately after placement of the tunnel section, once a week during the first month after placement and once a month from then on until stabilization of the construction. The concrete surface of the walls is scanned with an average lateral resolution of 5 mm. During the research until now, a workflow to determine the deformations of the tunnel sections is developed for processing the data with one laser scan software package (Trimble Realworks), followed by further analysis with a CAD software. The comparison between the successive measurements is based on the determination of the section radius every 0.1 grad. The differences that are determined between the different points in time show a stabilization of the construction after the second control measurement. The comparison of the second control measurement with the previous control measurement shows a systematic and random error of less than 1 mm. Different types of laser measurement instruments are used (pulse-based and phase-based laser scanner, robotic total station with scan function) and of each type the experimental standard deviation on the measurements is determined. Further improvement and extension of the workflow, research on the general trends that occur in the deformations of the different sections of the tunnel and research on the correlation between the measured tunnel deformations and simultaneous measured tension measurements is planned in the near future.

High Resolution Terrestrial Laser Scanning for Tunnel Deformation Measurements

Timothy NUTTENS, Alain DE WULF, Lander BRAL, Bart DE WIT, Leen CARLIER, Marijke DE RYCK, Cornelis STAL, Denis CONSTALES, Hans DE BACKER, Belgium

1. INTRODUCTION

Next to applications in the field of cultural heritage and archaeology, terrestrial laser scanning is also becoming an alternative for geodetic deformation measurements of civil constructions such as tunnels. The need for the acquisition of accurate (mm-level accuracy) 3D data with a very high point density in a very short time frame (up to 1 million points per second can be measured) and in sometimes very rough field conditions results in growing applications of laser scanning (Beraldin *et al.*, 2000; Biosca & Lerma, 2008). (Terrestrial) high resolution laser scanning delivers millions of 3D points with mm-accuracy, even in situations where other topographical techniques are difficult or impossible to use. Nevertheless, the price of the equipment and the still developing processing algorithms for the automatic processing of the very large 3D point clouds are a bottleneck to use laser scanning in many projects (Hesse & Stramm, 2004). Static terrestrial high resolution laser scanning is very suitable to efficiently develop 3D models of monuments, heritage buildings and civil technical constructions such as tunnels (Henriques & Casaca, 2006; Yoon *et al.*, 2008). A laser scanner records millions of 3D points in a very limited time schedule and this very dense point cloud represents an accurate '3D model' of the geometrical features of the object (Haala & Alshawabkeh, 2006). In the frame of this research, laser scanning is being used for the deformation measurements of a newly built railway tunnel (Zaventem, Belgium - Diabolo Project).

Where digital photogrammetry is not obvious or possible in these extreme conditions (e.g. little place on the tunnel drilling machine), laser scanning is applicable in these difficult situations. Measurements with a total station could also be an option, but the advantage of laser scanning is that millions of points of the complete monitored tunnel section are measured, where measurements with a total station focus on a rather limited number of specified points of the section to be closely monitored. In the following paper, one section of the tunnel will be discussed as 'model section', considering the error values during processing and the final determination of the deformations of the tunnel section. The results that are presented in this paper are the results of measurements with a terrestrial high resolution Time-of-Flight laser scanner Leica ScanStation 2 (measurement immediately after placement until control measurement 4), a phase-based scanner Leica HDS6100 and a one-man robotic total station Trimble S6 with scan function (control measurement 5 and 6). The experimental standard deviation is determined for these three types of measurement instruments.

2. DIFFERENT TYPES OF LASER SCANNERS

In general, there are two types of laser scanners that are based on the principle of time measurement: phase-based laser scanners and pulse-based scanners (Time-of-Flight). Pulse-based laser scanners (e.g. Leica ScanStation 2, Trimble GX) are based on emitting pulses of a laser beam and picking up the reflection of these laser pulses onto an object. When the time delay between emitting and receiving of the laser pulse is very accurately measured, the distance between the laser scanner and the measured point can be determined. Together with the horizontal and vertical angles that are registered in the instrument, the accurate 3D coordinates of each measured point can be determined. The restriction with this type of laser scanner is that the time delay that is measured has to be longer than the width of the laser pulse to avoid interfering measurements of different points. Time-of-Flight laser scanners have a scan distance up to 200 till 700 m, with a scan speed up to 50 000 points per second (Figure 1).

Laser Scanning System	
Type	Pulsed; proprietary microchip
System Performance	
Accuracy of single measurement	
Position*	6 mm
Distance*	4 mm
Angle (horizontal/vertical)	60 µrad/60 µrad, one sigma
Range	300 m @ 90%; 134 m @ 18% albedo
Scan rate	Up to 50,000 points/sec,
Scan resolution	
Spot size	From 0 - 50 m: 4 mm (FWHM - based); 6mm (Gaussian - based)
Field-of-view (per scan)	
Horizontal	360° (maximum) ¹
Vertical	270° (maximum) ¹

Laser Scanning System	
Type	Phase-shift
System Performance	
Accuracy of single measurement	
Position*	5 mm, 1 m] to 25 m range; 9 mm to 50 m range
Distance*	≤2 mm at 90% albedo up to 25 m; ≤3 mm at 18% albedo up to 25 m; ≤3 mm at 90% albedo up to 50 m; ≤5 mm at 18% albedo up to 50 m
Angle (horizontal/vertical)	125 µrad/125 µrad, one sigma
Range	79 m ambiguity interval 79 m @90%; 50 m @18% albedo
Scan rate	Up to 508,000 points/sec, maximum instantaneous rate
Scan resolution	
Spot size	3 mm at exit (based on Gaussian definition) + 0.22 mrad diverg 8 mm @25 m; 14 mm @50 m
Field-of-view	
Horizontal	360° (maximum)
Vertical	310° (maximum)
Aiming/Sighting	Optical horizontal sighting using QuickScan™ feature

Figure 1: Specifications of Leica ScanStation2 (pulse-based laserscanner) (Example Left) - Leica HDS6100 (phase-based laserscanner) (Example Right)
(Source: <http://www.leica-geosystems.com/>, 2009)

Phase-based laser scanners (e.g. Leica HDS6100, Faro Photon 120) are not based on laser pulses, but on a continuous laser beam. The phase difference between the laser beam that's emitted from the scanner and the received reflection of this laser beam is then determined. From this phase difference, a time delay between the emission of the laser beam and the reception of the reflection can be calculated. This time delay, multiplied by the laser light propagation speed, represents the distance to the object. A combination of this distance with the registered horizontal and vertical angles of the emitted laser beam leads to the 3D coordinates of the scanned points. Phase-based scanners have typically a shorter range (scan distance up to 120 m) than pulse-based scanners, but a much higher scan speed (up to 1 million points per second) and a higher accuracy at short distances (i.c. maximum 8 m) (Lerma Garcia et al., Pfeifer & Briese, 2007) (Figure 1).

PERFORMANCE

Angle measurement	
Accuracy (Standard deviation based on DIN 18723)	2" (0.5 mgon)
Angle reading (least count)	
Standard	1" (0.1 mgon)
Tracking	2" (0.5 mgon)
Averaged observations	0.1" (0.01 mgon)
Automatic level compensator	
Type	Centered dual-axis
Accuracy	0.5" (0.15 mgon)
Range	±6' (±100 mgon)
Distance measurement	
Accuracy (S. Dev.)	
Prism mode	
Standard	±(3 mm + 2 ppm) ±(0.01 ft + 2 ppm)
Tracking	±(10 mm + 2 ppm) ±(0.032 ft + 2 ppm)
DR mode	
Standard measurement	±(3 mm + 2 ppm) ±(0.01 ft + 2 ppm)
Tracking	±(10 mm + 2 ppm) ±(0.032 ft + 2 ppm)
>300 m (656 ft)	
Standard measurement	±(5 mm + 2 ppm) ±(0.016 ft + 2 ppm)

Figure 2: Specifications of One-man Robotic Total Station Trimble S6 (2" DR 300+)
(Source: <http://trl.trimble.com/>, 2009)

The measurements of the tunnel sections are not only done by the above-mentioned types of laser scanners, but also with a one-man robotic total station Trimble S6 (2" DR300+) with scan function (Figure 2). The fact that there are similar point clouds scanned with different types of measurement instruments, allows on the one hand to determine the (experimental) standard deviation of these different measurement instruments in comparable environmental conditions and on the other hand to compare the results and the achievable accuracies of the deformation measurements taken by the different measurement instruments.

In this phase of the research, the experimental standard deviations of all three types of scanning instruments have been determined. The conditions in which the standard deviation is determined is similar for all three instruments. One section is scanned four times, both from the left scanning position and the right scanning position within a time frame of two to four hours. The scan position for all four measurements remained unchanged. The tunnel bracket is not taken off the tunnel section and put back on between the measurements. The processing of these point clouds (below) is performed by a fixed workflow, so that the results of the different measurements and the different scanning instruments can be compared with each other. The workflow is further specified and detailed below. For one scanning instrument, the four measurements allow to calculate an experimental standard deviation for this instrument, in these specific environmental conditions. A value for the radius of the cross-section is calculated every 0.1 grad, so for each 0.1 grad -based on the four measurements- a standard deviation is determined. The average of these 4000 standard deviations (one for each 0.1 grad) gives a value for the general experimental standard deviation (1σ) of the scanning instrument (Figure 3).

Scanning instrument	Experimental Standard Deviation (mm)
Leica ScanStation 2 Pulse-based Laser scanner	1,6
Leica HDS6100 Phase-based Laser scanner	0,4
Trimble S6 Robotic Total Station	0,8

Figure 3: Summary of experimental standard deviations (1σ) of the different types of measurement instruments used (Source: Own research, 2009)

3. DEFORMATION MEASUREMENTS OF THE TUNNEL SECTIONS

3.1 Scanning of the tunnel sections

The measurements as part of this research are carried out at the construction site of two railway tunnels that are being built in Zaventem (Belgium) to give the National Airport (Brussels Airport) a better connection to the North (Diabolo project - NV Infrabel¹). The tunnels are approximately 1.1 km long and have, according to the design, a inner diameter of 7.300 meter. Divided over the two tunnels that are being built (one for each direction of the train traffic), twelve critical sections are measured on a regular base with laser scanning. Each tunnel section is 1.5 m wide (measured in the direction of the longitudinal axis of the tunnel) and is made out of seven concrete plates and one closing concrete plate.

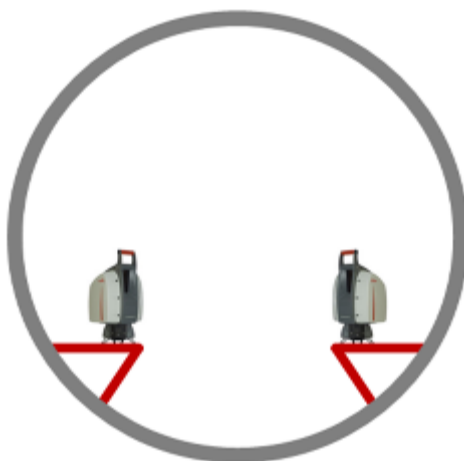


Figure 4: Approximate set-up of the two scanning positions for each tunnel section (Source: Own research, 2009)

¹ http://www.infrabel.be/portal/page/portal/pgr_inf2_e_internet/mobility_project/le_projet_diabolo

The monitored sections are measured a first time immediately after the placement, in the head of the tunnel drilling machine. This means that the complete recording of the point cloud is completed within two hours after placement. After this first measurement, the sections are scanned once a week during the first month after placement and from then on once a month until stabilization of the tunnel section. When no significant difference can be determined between the last control measurement and the previous control measurement, the term 'stabilization of the construction' can be used.

Due to obstacles in the tunnel, there are two scanning positions needed to scan one tunnel section, one position on the left side of the tunnel and one on the right side (Figure 4). During the measurements right after the placement of the tunnel section that has to be monitored, the tunnel drilling machine is obstructing part of the section, seen from one scan position. By scanning from the second scan position, the coverage of the section is completed. During the following monitoring measurements, a pathway, pipes, a ventilation shaft and temporary train rails are causing some 'blind spots' on the tunnel section where no measurements can be made. On the two scanning positions of one tunnel section, the laser scanner is mounted on a tunnel bracket (Type 14-TK500 Goecke), which is attached to the tunnel wall with four concrete bolts (Fischer FBN II 10/20 - 10x96 mm), and placed horizontally (Figure 5).



Figure 5: Laser scanner mounted on a tunnel bracket attached to the concrete tunnel section (Source: A. De Wulf, 2009)

The concrete surface of the tunnel sections is scanned with an average lateral resolution of 5 mm (horizontally and vertically). The total point cloud of one section is up to five million points (Leica ScanStation 2) or 40 million points (Leica HDS 6100). The cross-sections that are discussed in this paper are scanned with the Leica ScanStation 2 laser scanner. After filtering the non-relevant points, the point cloud is used to model the tunnel section and determine the cross-section. To register both scanning positions, at least ten to twelve targets (Trimble targets as well as Leica targets) are permanently attached to the tunnel wall with special concrete glue (*TEC7 Super7 Plus + Activator*). Both types of targets are shown in Figure 6.

The Trimble targets are made out of a low reflective background (dark green) (15 x 15 cm) with in the centre a high reflective circle with a diameter of 6.8 cm. The Leica targets are composed of a circle divided in quadrants, with an alternating white and black quadrant. The use of two types of targets allows to develop a workflow for different software packages (Leica Cyclone, Trimble Realworks or a third-party software), to compare these workflows and to determine the most efficient workflow and software package and determine differences in achievable accuracies.



Figure 6: Trimble Target (Upper example) - Leica Target (Lower example)
(Source: A. De Wulf, 2009)

3.2 Processing of the laser scan point cloud

A workflow to determine the deformations of the tunnel sections has been developed for the processing of the data with the Trimble Realworks software, followed by further processing of the data with CAD software. This workflow to extract a cross-section from a point cloud of a tunnel section, followed by the determination of the differences between this cross-section and the design of the tunnel dimensions and previous measurements will be detailed hereunder.

The point clouds of each scan position (two scan positions for each tunnel section) are first filtered. They contain a lot of non-relevant points such as scanned obstacles in the tunnel or points of the neighboring tunnel sections. After the filtering, the relative orientation of both point clouds (one point cloud from each scanning position) is performed. This orientation is a target-based registration, which means that both point clouds are linked together based on the overlapping scanned targets of the tunnel section. The targets were positioned on the tunnel section, in such a way that there are at least three overlapping targets to orient the point

clouds. To avoid any problems during the processing of the 3D point cloud data, there is opt for at least four to five overlapping targets between the two point clouds. The residual error on the orientation of the left and right point cloud for the different measurements (the measurement immediately after placement, the control measurements) lies, for the tunnel section discussed in this paper, between 0.56 mm and 1.45 mm, using five common targets for the left and right scan position.

When the point clouds of both scan positions are filtered and oriented, a best-fit cylinder is created through this complete point cloud. The radius of this best-fit cylinder is determined by the software. The radius is not fixed in advance by the operator, because this actual radius of the tunnel section can be slightly different from the design radius value. The theoretical radius of this cylinder (as determined on the design plans) is 3.6500 m. The axis of this best-fit cylinder is the base for the determination of the final cross-section. The cross-section is taken perpendicular to the axis of this cylinder, after a TIN (triangulated irregular network) mesh is being created through the point cloud. This mesh is created based on the 3D coordinates of the point cloud of the tunnel section, but the gaps that may occur in the filtered point cloud are not filled by the software. Those gaps can be formed by large obstacles in front of the tunnel section, where no points can be scanned, or during the processing of the point cloud data, where the operator has removed the points of the notches in the concrete plate. The concrete plates of a tunnel section have a couple of notches where the bolts to hold the adjacent sections together are attached, which have to be deleted for a correct determination of the best-fit cylinder. By defining the cross-section through a mesh, the result is a polyline, which can be exported to a CAD software for further analysis and plan plotting.

To be able to analyze the measurements and the cross-sections of the specified tunnel section on different points in time, the cross-section of the tunnel section, based on the scans made on those different points in time (once immediately after placement, once a week during the first month and then once a month until stabilization), is always determined through the same target, the so-called 'reference target'. This way, it's made sure that for each control of a tunnel section, the cross-section is located on the very same place of the tunnel section.

3.3 Analysis of the cross-section

After the cross-section is determined in the laser scan software package (i.c. Trimble Realworks), a further analysis of this polyline is performed in CAD software to determine the differences between this specific cross-section and the design of the tunnel section and previous control measurements. During this further analysis in the CAD software, 4000 lengths from the center of the cross section to the polyline are calculated. A radius of the cross-section is so determined every 0.1 grad.

These 4000 values for the radius of the cross-section are then smoothed by replacing every radius value by the average of this radius and the twenty-five previous and the twenty-five following values. This means that every radius value is replaced by the average of the fifty-one adjacent values, so an average radius is computed over a five grade area or ca. 29 cm of

the tunnel surface. The aim is to flatten out 'higher' frequency deviations in the measurements, as it is not expected that a concrete element itself will show any measurable deformation. An important point is the question whether or not the applied five grade smoothing is not excessive and gives a false 'optimistic' image of the standard deviation. Therefore, the processing was repeated without smoothing for the first two measurements of a section. The smoothing, as expected, has an effect on the computed standard deviations, that are slightly higher without smoothing (0.2 - 0.3 mm), but that effect is not excessive. The amplitude of the non-smoothed data is also limited. The smoothing yields clearer drawings without 'masking' excessive measurements and without influencing the significance levels of the deviations measured. Where certain parts of the tunnel section cannot be measured -due to obstacles that block the laser beam-, the smoothed value of the radius will be the average of less than fifty-one adjacent values, because not all adjacent values are determined in this case. Based on these (smoothed) measurements, the deformations of the cross-section, compared to the original design dimensions and previous measurements of the tunnel wall, are determined.

Laser scan measurement immediately after placement	Differences compared to the theoretical design (radius: 3.6500 m)	
(Temp.: 23 °C)		
(Air Humidity: 66 %)		
Systematical Error (mm)	-0.4	
(Average of algebraic values)		
Random Error (mm)	3.9	
(Average of absolute values)		

Table 1: Differences between the measurement immediately after placement and the theoretical design (Source: Own research)

Control measurement 1	Differences compared to the theoretical design (radius: 3.6500 m)	Differences compared to the measurement after placement
(Temp.: 18 °C)		
(Air Humidity: 70 %)		
Systematical Error (mm)	-3.6	-2.7
(Average of algebraic values)		
Random Error (mm)	7.6	6.5
(Average of absolute values)		

Table 2: Difference between the first control measurement after 1 week and the theoretical design and the previous measurement (Source: Own research)

Table 1 shows the differences between the laser scan immediately after placement of the tunnel section and the theoretical design of the section. Hereby are the smoothed radius values that are determined every 0.1 grad from the cross-section of the point cloud compared to the theoretical radius, which is 3.6500 m. The average of the algebraic values of these differences (-0.4 mm) represent the systematic error (bias in the measurement), whereas the average of the absolute values (3.9 mm) represents the random error (noise of the measurements) of the tunnel radius “as-built”, including the measurement errors.

The differences between the first control measurement, the theoretical design and the measurement immediately after placement are shown in Table 2. Compared to the theoretical design, the systematic error is -3.6 mm and the random error is 7.6 mm. These values are higher than the systematic error (-2.7 mm) and random error (6.5 mm) of this control measurement compared to the measurement after placement. This increase in differences is most probably due to the jet grouting (cement injection) by the tunnel drilling machine, which causes a enormous external pressure on the concrete tunnel sections. After this pressure, the sections are settled in their final position, as following tables also indicate. When scanning the tunnel section on different points in time, it is not possible to scan the complete tunnel section each time and the blind spots due to obstacles in the tunnel may differ for the different successive control measurements. These changing scanning conditions lead to calculated differences between following control measurements that may deviate from values that can be expected.

Control measurement 2 (Temp.: 20 °C) (Air Humidity: 63 %)	Differences compared to the theoretical design (radius: 3.6500 m)	Differences compared to the measurement after placement	Differences compared to the previous control measurement
Systematical Error (mm) (Average of algebraic values)	-3.5	-2.5	0.2
Random Error (mm) (Average of absolute values)	6.8	5.9	1.4

Table 3: Differences between the second control measurement after 2 weeks and the theoretical design and the previous measurement (Source: Own research)

Control measurement 3 (Temp.: 18 °C) (Air Humidity: 82 %)	Differences compared to the theoretical design (radius: 3.6500 m)	Differences compared to the measurement after placement	Differences compared to the previous control measurement
Systematical Error (mm) (Average of algebraic values)	-3.5	-2.4	0.2
Random Error (mm) (Average of absolute values)	6.9	5.9	0.9

Table 4: Differences between the third control measurement after 3 weeks and the theoretical design and the previous measurement (Source: Own research)

Table 3 and Table 4 represent the differences between control measurement 2, respectively 3, and the theoretical design, the measurement after placement and the previous control measurement. The systematic error between control measurement 2 and the theoretical design (-3.5 mm), the measurement after placement (-2.5 mm) and the first control measurement (0.2 mm) are very similar to the respective values on the third control measurement (respectively -3.5 mm, -2.4 mm, 0.2 mm). When the random errors of the second (6.8 mm - 5.9 mm - 1.4 mm) and third control measurement (6.9 mm - 5.9 mm - 0.9 mm) are compared, there are also only minimal differences. These values let us conclude that the differences between the control measurements of this tunnel section decrease and that stabilization of the tunnel section appears to be obtained.

The tunnel sections are monitored up to three months after the placement, which makes that there are in total six control measurements. The following control measurements (up to control measurement six) show similar differences between the scans and respectively the design dimensions, the measurement after placement and the previous control measurement. The last two control measurements were scanned with the robotic total station Trimble S6, but the results of the comparison of measurements with this measurement instrument and the Leica ScanStation 2 laser scanner are similar to the comparison of previous control measurements. The statement of stabilization of the tunnel section is confirmed by these control measurements.

The differences between the measurement immediately after placement of the tunnel section and the theoretical design is also represented in the following figure (Figure 7). The theoretical design of the tunnel section is a circle with a radius of 3.6500 m. The measurement after placement is indicated by the black line in the middle. The two boundary (blue) lines indicate the interval of two times the experimental standard deviation (2σ). The differences between this theoretical design and the measured cross-section are 100 times exaggerated. The true values of the differences are indicated approximately every 20 grad. The X-axis is pointing horizontally to the right (when looking away from the entrance of the construction site), the Y-axis is pointing vertically. The Z-axis follows the longitudinal axis of the tunnel.

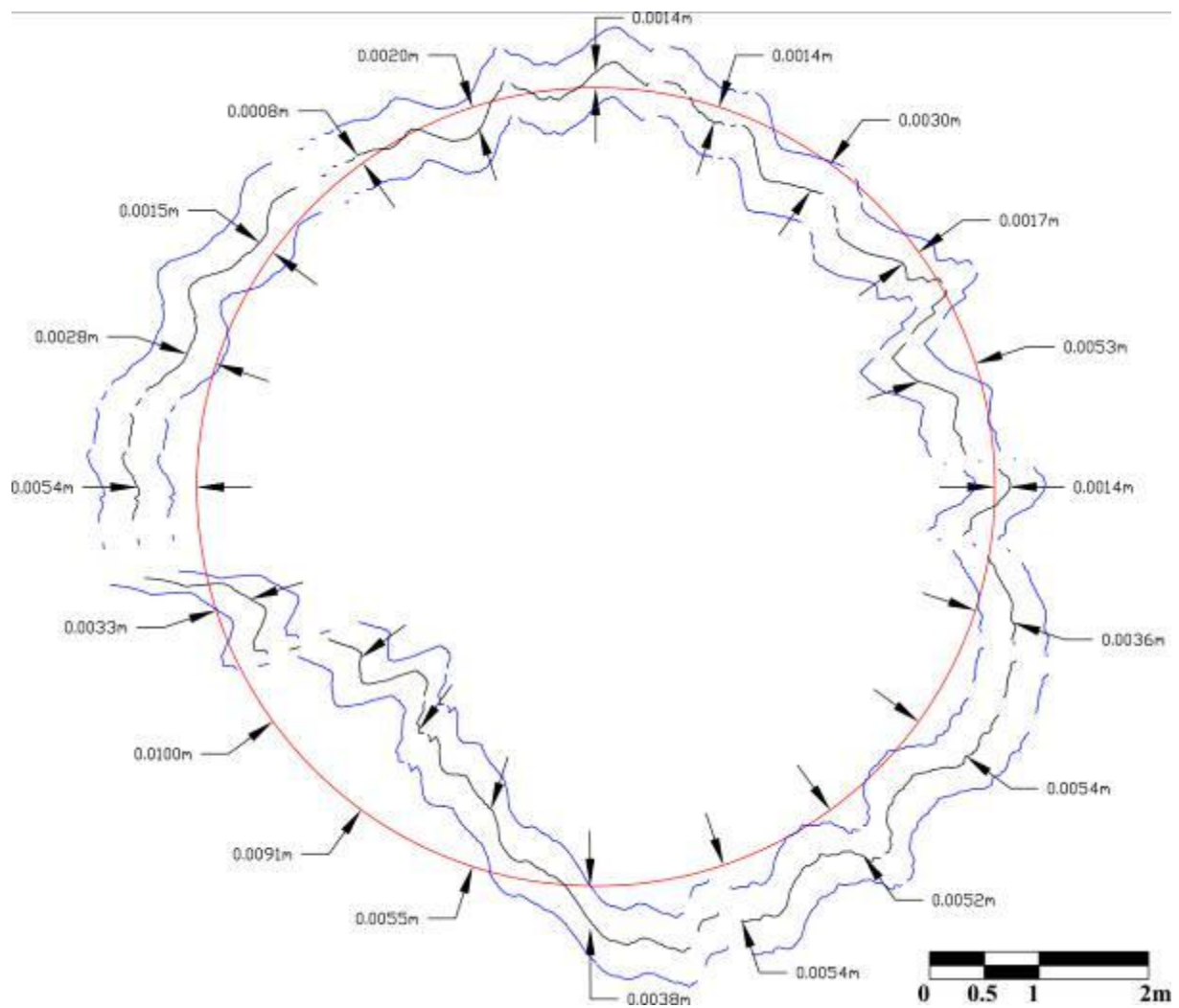


Figure 7: Theoretical design of the tunnel section (red circle); the cross-section immediately after placement of the section (black middle line) and 2σ (blue boundary lines) – the differences are drawn 100 times exaggerated (Source: Own research)

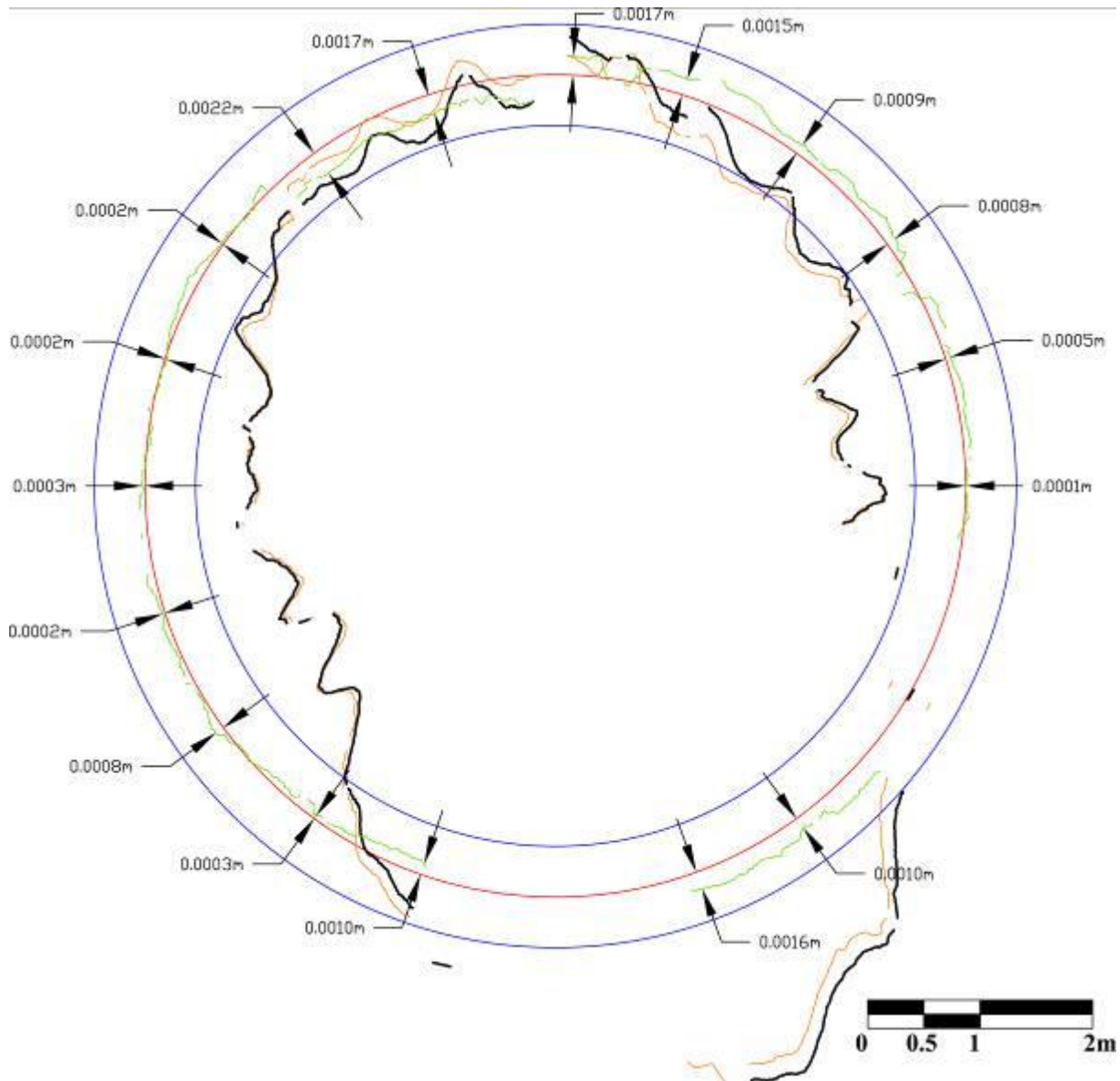


Figure 8: Control measurement 2 (orange/dark gray); Control measurement 3 (black); difference between control measurement 2 and 3 in regard to the design (green/light gray) – the differences are drawn 100 times exaggerated (Source: Own research)

The above figure (Figure 8) shows both control measurement two and three (respectively the orange/dark gray line and black line). All deformations are 100 times exaggerated. The difference between both control measurements is indicated by the green line. These differences are again 100 times exaggerated and are set out in reference to the design of the tunnel section (red circle with radius 3.6500 m). The dimensions represented on the plan are the real values of the deformations between the second and the third control measurement. As clearly shown on the plan, all those differences are smaller than the interval of $2\sigma\sqrt{2}$ or 4.5 mm. There are no significant deformations anymore in this stage of the tunnel construction.

4. FUTURE RESEARCH

Research in the following months will focus on the optimization of the developed workflow and the determination of an experimental standard deviation for different types of laser scanners in the situation where the tunnel bracket is removed and put back on the section. By removing and reinstalling the tunnel bracket in the time span between the four following measurements used to determine the standard deviation, a better idea will be obtained concerning the stability of the scanning position that influences the accuracy of the measurements. Another focus in the following research will be improving the relative orientation of the two complementary scanning positions.

To get a detailed view on the specifications of the used type of laser scanner, different experiments are planned in the foreseeable future, such as defining the standard deviation of a fitted geometry through a point cloud. Various materials (very high reflective - low reflective) and different angle positions of this geometric object will be tested. Also other software packages for the processing of laser scan data are being tested and compared with the results of the Trimble Realworks software. Research on the correlation between the measured tunnel deformation and simultaneous measured tension measurements is also planned for the near future.

5. CONCLUSION

The results of the accuracies obtained by the application of laser scanning in the difficult field conditions of a railway tunnel that is being built are within tolerances. The determined accuracies and differences between the laser scan measurements of monitored tunnel sections right after placement, once a week during the first month and then once a month until stabilization are clearly confirmed by later measurements of the same tunnel sections and of the other monitored tunnel sections. The differences calculated between the different measurements in time, indicate a stabilization of the tunnel section after the second control measurement, thus two weeks after construction of that tunnel section. From that point in time, the systematic and random error between the following and previous control measurement are less than 1 mm and non significant statistically.

REFERENCES

Beraldin J, Blais F, Boulanger P, Cournoyer L, Domey J, El-Hakim SF, Godin G, Rioux M, Taylor J, 2000, Real world modeling through high resolution 3D imaging of objects and structures, *ISPRS Journal of Photogrammetry & Remote Sensing* 55 (2000), pp. 230-250.

Biosca J, Lerma JL, 2008, Unsupervised robust planar segmentation of terrestrial laser scanner point clouds based on fuzzy clustering methods, *ISPRS Journal of Photogrammetry and Remote Sensing* 63 (2008), pp. 84-98.

Haala N, Alshawabkeh Y, 2006, Combining laser scanning and photogrammetry – A hybrid approach for heritage documentation, In: *Proceedings of CIPA/VAST/EG/EuroMed 2006:*

37th CIPA International workshop dedicated on e-documentation and standardization in cultural heritage, Eurographics, Aire-la-Ville, Switzerland, ISBN 3905673428.

Herniques MJ, Casaca J, 2006, Uncertainty in tacheometric measurement of convergences in tunnels, 3rd IAG / 12th FIG Symposium, Baden, May 22-24, 2006.

Hesse C, Stramm H, 2004, Deformation measurements with laser scanners. Possibilities and challenges, International Symposium on Modern Technologies, Education and Professional Practice in Geodesy and Related Fields, Sofia, 04-05 November 2004, pp. 228-240.

Lerma Garcia JL, Santana Quintero M, Heine E, Ed., Application of Terrestrial Laser Scanning for Risk Mapping, Editorial Universidad Politecnica de Valencia, 2007, Valencia, ISBN 978-84-8363-199-7.

Pfeifer N, Briese C, 2007, Laser scanning – Principles and Applications, GeoSiberia 2007, International Exhibition and Scientific Congress, April 2007.

Yoon J, Sagong M, Lee JS, Lee K, 2009, Feature extraction of a concrete tunnel liner from 3D laser scanning data, NDT&E International 42, 2009, pp. 97-105.

CONTACTS

Timothy NUTTENS
Ghent University - Department of Geography
3D Data Acquisition Cluster
Krijgslaan 281 (Building S8)
B-9000 Gent
BELGIUM
Tel. +32 9 264 46 56
Fax +32 9 264 49 85
Email: Timothy.Nuttens@UGent.be
Web site: <http://geoweb.ugent.be/data-acquisition-3d>